A STATISTICAL STUDY OF THE BEHAVIOR OF THE AFTERSHOCK SEQUENCE DUE TO JUNE 1, 2019 KORÇA (M_L=5.3), SOUTHEASTERN ALBANIA, EARTHQUAKE

Rrapo ORMENI
Institute of Geosciences, Energy, Water and Environment, Polytechnic University of Tirana, Albania
Serkan ÖZTÜRK
Gümüşhane University, Department of Geophysics, 29100, Gümüşhane, Turkey

---

ABSTRACT

The present paper estimates the number of the aftershocks that the main shock produces and forecasts the occurrence probability of specific aftershocks. An aftershock probability model involving the Gutenberg-Richter and modified Omori scaling laws was employed for the evaluation of the mainshock-aftershock pattern. Here, a statistical analysis of the aftershock sequence of June 1, 2019 earthquake, (M_L5.3), occurred in Korça, southeastern Albania, was achieved. So, 719 aftershocks occurred in about 110 days, between June 1, 2019 and September 19, 2019, and with $M_L \geq 0.6$ were used. Mcomp was taken as 1.8, and the b-value of the Gutenberg-Richter relation was estimated as 0.81±0.07. Temporal decay parameters of the modified Omori law were calculated as p=0.96±0.04, c=0.134±0.047 and K=69.46±7.42 with Mcomp≥Mmin=1.8, and the time elapsed since mainshock is nearly 0.0014 day. A b-value lower than 1.0 might be interpreted as a higher stress distribution to be built up over time and to be released by future mainshocks. If the p-value is smaller than 1.0, the decay rate of the aftershock occurrences is low. Dc-value was calculated as 1.89±0.07 showing that aftershocks have homogeneous distribution at larger scales in smaller areas. Probability for the maximum aftershock magnitude of 5.0 was estimated as 11.93 % and the expected number of aftershocks for the magnitude level of 2.5 was calculated as 14.25. Thus, space-time-magnitude assessments of the aftershock sequence show that statistical behaviors of aftershock occurrences may supply preliminary results on the aftershock probability evaluation and aftershock hazard in Korça, Albania.

***Keywords*:** Albania, Gutenberg-Richter, Modified Omori, fractal dimension, aftershock hazard

1. INTRODUCTION

The Institute of Geosciences, Energy, Water and Environment (IGEWE) recorded a strong earthquake of M_L=5.3 with epicenter located near Floq village, 13 km south-southwest of Korça, Albania. The epicenter coordinates are 40.462^{o}N and 20.723^{o}E, 130 km southeast of Tirana and near the border with Greece. The earthquake has been recorded at a shallow depth of 2.8 km. The event was detected on June 1, 2019 at 04:26:17 UTC. Table 1 reports detailed information about the earthquake occurrence. The maximum (Ma_{max}) and minimum (Ma_{min}) magnitudes of aftershock sequence are also given. The mainshock was subsequently followed by a series of weaker aftershocks. The largest magnitude of M_L=5.0 was recorded a few hours later from mainshock. Buildings were damaged and three people were injured within three hours. Throughout the region, including the municipalities (towns and villages) of Korça, Kolonja and Devolli districts, a total of 688 residential houses were damaged. 130 out of 688 residential houses sustained major damages becoming uninhabited, 248 suffered substantial damages, and the remainder sustained minor damages. Albania and the boderging countries have suffered from some moderate earthquakes. Here we can mention the earthquake of October 15, 2016 (*M*5.6) in the bordering area between Greece and Albania, July 3, 2017 (M5.2) in the bordering area between Macedonia-Albania, and the earthquake of July 4, 2018 in Durrës (M5.1) which result in human victims and enormous material loss. Earthquakes events are common in this part of the world as the African Plate moves northward towards Europe by 4-10 mm annually, with regular earthquakes occurring alongside the Eurasia-Africa plate boundary, mainly in Turkey, Greece, Sicily and Italy.

Table 1. The earthquake data

Year	Month	Day	Origin Time (UTC)	Longitude	Latitude	Depth (km)	(M_L)	Ma_{max}	Ma_{min}
2019	06	01	04:26:17	20.723	40.462	14	5.3	5.0	0.6

Sulstarova and Kociaj (1975), Aliaj *et al*., (2000; 2010), and Aliaj and Meco (2018) stated that Korça region and the surrounding experienced some strong and large earthquakes. In addition, this region has been characterized in the last century by earthquakes causing death among the population and significant material damages. The strong earthquakes that hit this area in the 19th century are the earthquake dated in July 4, 1878, I=VII (front MSK-64), and the earthquake of June 2, 1896, I=VIII (front MSK-64). In the last century, the Korça area has been hit by several earthquakes such as the earthquake of January 28, 1931, M_S=5.8, and with epicenter located in Korça

(Sulstarova and Kociaj 1975), the earthquake of May 26, 1960, M_S=6.4, and with epicenter located in Korça (Sulstarova and Kociaj 1975). Ormeni and Dushi (2009) said that the latest earthquake that affected the area around Korça is the earthquake of August 28, 2008 with the epicenter located in Voskopoja (Korça), and magnitude M_S=4.3.

Appropriate assessment of earthquake hazard helps minimize human loss and any kind of damage and disruption. Therefore, analyses of aftershock occurrences may give some significant and preliminary perspective for the seismic hazard. Statistical and physical analyses of aftershock occurrences have been carried out by different authors for different aftershock sequences and some important results have been provided for specific aftershock areas (Utsu 1961; 1971; Vere-Jones 1975; Sulstarova and Lubonja 1983; Sulstarova 1985; Muço 1993; Wiemer and Katsumata 1999; Felzer *et al*., 2003; Helmstetter and Sornette 2003a; Ogata 2001; 2010; Enescu and Ito 2002; Bayrak and Öztürk 2004; Kociu 2005; Narteau *et al*., 2005; Daniel *et al*., 2006; Öztürk *et al*., 2008; Öztürk and Ormeni 2009, Aliaj *et al*., 2010; Ormeni *et al*., 2011; Scherbakov *et al*., 2013; Chan and Wu 2013; Ávila-Barrientos *et al*., 2015; Hainzl *et al*., 2016; Shebalin *et al*., 2017; Zhuang *et al*., 2017; Marsan and Helmstetter 2017; Wei-Jin and Jian 2017; Öztürk and Şahin 2019; Ormeni and Öztürk 2018; 2019). Aftershock probability evaluation refers to statistically expressing and estimating the frequency that an aftershock of a specific magnitude will occur. The modified Omori method (Utsu 1961) estimates the aftershock numbers that can occur from the mainshock, but combining this method with the Gutenberg-Richter (Gutenberg and Richter 1944) law for a probability evaluation of aftershock occurrences would be of great benefit. In addition, fractal dimension of aftershock epicenter distributions is an effective tool to describe the self-similar structure of aftershock occurrences and fractal dimension has widely been used in statistical seismology, especially for the measurements of complexity in the aftershock occurrence and aftershock clustering (Öncel *et al*., 1996).

Physics of the earthquake process depends on the stick-slip motion occurring on a fault plane and concludes a specific seismic energy. However, in reality, nearly all of the strong/large seismic mainshocks may trigger numerous small to moderate events within a short period of time, known as aftershocks. Based on the Båth's Law, Helmstetter and Sornette 2003(b) said that in an aftershock sequence, the magnitude of the largest event is typically assumed to be about one magnitude smaller than the magnitude of the mainshock. Nevertheless, in a typical aftershock sequence, the total seismic energy released by the aftershocks is actually ~10 times smaller than of the mainshock (Lay and Wallace 1995). Also, the co-seismic fault geometry strongly controls the regional aftershock elongation (Nemati 2014). It is well

known that strong/large aftershocks can cause additional cumulative damage to structures. As the aftershocks are hard to be predicted, hazard estimation based on the aftershock probability would be of great importance and investigation of the influence recorded mainshock-aftershock seismic sequences on the dynamic response and accumulated damage of structures would be of immediate importance. Thus, identification of area for aftershocks dispersal becomes very important.

There is a significant attention paid to aftershock occurrences in recent years. Aftershock sequences can provide an understanding of the mechanism of earthquakes and they are potential sources of information about earthquakes nucleation and the physical characteristics of materials in fault segment inside which slip occurs during an earthquake (Hamdache *et al*., 2013). Hence, many statistical models have been provided to describe aftershock properties in space, time and magnitude. These studies generally focus on the analysis of two seismicity parameters: the *b*-value of the magnitude-frequency distribution, and the *p*-value, explaining the temporal decay rate of aftershocks, as well as *Dc*-value describing regional features of the aftershock sequences. Consequently, the present paper aims to: i) provide a detailed space-time-magnitude analysis including several aftershock parameters such as the *b*-value of the frequency-magnitude distribution, the *p*-value of the modified Omori law and *Dc*-value of the fractal dimension for 719 aftershocks identified in 110 days after the mainshock and, ii) provide a probability evaluation on the aftershock occurrence based on the combination of the Gutenberg-Richter and modified Omori formulas to forecast the number of large aftershocks might follow the main shock, and to make an aftershock probability assessment for a randomly chosen event that is larger than or equal to specific aftershock size. In this context, we realized an aftershock probability evaluation for the aftershock sequence of June 1, 2019 earthquake (M_L=5.3), in which occurred near Korça, Albania.

2. Definition of Aftershock Data of July 1, 2019 Korça Earthquake

In the present investigation, the aftershock sequence of June 1, 2019 earthquake, near Korça town of Albania was used for the aftershock probability evaluation. The data here used have been collected from the Albanian seismological stations, AUTH (Greqi), INGV (Itali), MEDNET, and Montenegro networks. A complete and homogenous aftershock catalog was obtained for the Korça mainshock with local magnitude M_L=5.3, occurred at 40.462^{o}N and 20.723^{o}E, and at 4:26:17.0 UTC on June 1st, 2019. The aftershock sequence contains about a time interval of four months, that is from the time of the main event (June 1st, 2019) until September 19th, 2019. A total of 719 aftershocks with magnitude M_L larger than or equal to 0.6 were

used in a time period of 110 days. The epicenter distributions of aftershocks are in the Figure 1 depicted. The Figure 2a depicts the cumulative number of aftershocks in about a time interval of four months. In order to evaluate the magnitude variations as a function of time, time-magnitude analysis of aftershocks is in the Figure 2b depicted. Temporal changes of magnitudes for aftershock sequence were plotted in a time interval of about 110 days. As the Figure 2b depicts, the largest aftershock with M_L=5.0 occurred a few hours after the mainshock. However, occurrences of the aftershocks greater than M_L=3.0 show two increases; 26 and 59 days after the mainshock. There are also several aftershocks which magnitude varies between 4.0 and 5.0 in these days after the mainshock. These picks could also be seen in Figure 2a. There is a decreasing trend in the number of aftershocks with magnitude M_L=3.0 after the first two months from the mainshock, and magnitude of aftershocks mostly changes between 1.0 and 3.0 in the rest of aftershock period.

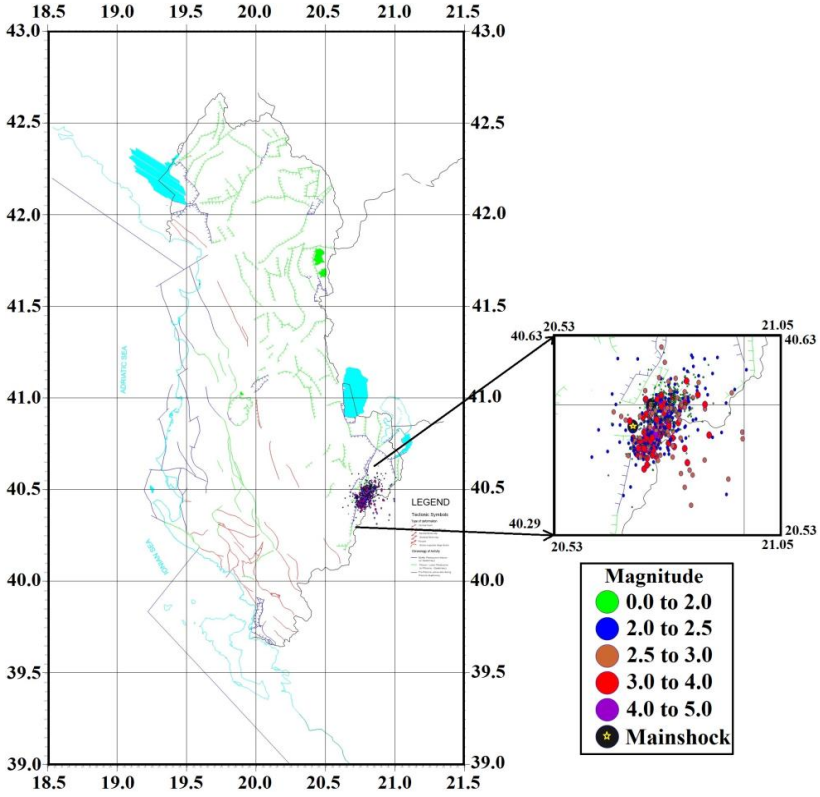

Fig. 1: Aftershock epicenter map of June 1, 2019 near Korça earthquake. Data from small to large magnitude level of the aftershocks were marked by different color and symbols.

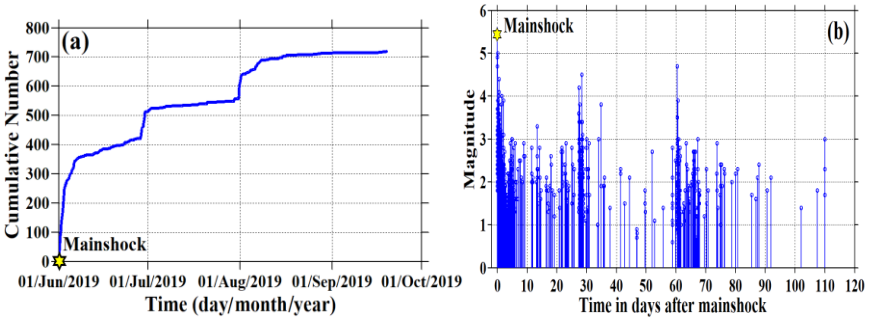

Fig.2:(a) - Cumulative number of aftershocks in about four months after the mainshock. (b)-Magnitude changes of aftershocks during 110 days after Korça earthquake of June 1, 2019.

Utsu (1961) said that it is a remarkable fact that the aftershocks show elliptical distribution that spread in different directions from the mainshock epicenter. Therefore, these shocks and subsequent events that fall in this region can all be described as aftershocks. Thus, a general description was given as "it is frequently observed that a number of events occur in a group within a limited interval of time and space and after the mainshock are called aftershocks." Also, many researchers suggested different time intervals for aftershock duration, from one month to one year (Utsu 1961; Wiemer and Katsumata 1999; Öztürk *et al*., 2008; Öztürk and Şahin 2019). We identified the region and time interval of Korça aftershocks by considering these literature studies.

3. Methodology and Aftershock Hazard Parameters

Statistical properties of aftershock occurrences might provide preliminary and reliable information about the fault structure, cracks distribution, earthquake migration and the state of stress in the crust (Öztürk and Şahin 2019). Although there are several ways to define the aftershock behaviors from a mainshock, aftershock characteristics have generally been described in space (fractal dimension, Grassberger and Procaccia 1983), time (modified Omori law, Utsu *et al*., 1995) and magnitude (Gutenberg-Richter law, Gutenberg and Richter 1944). These statistical models are the best known and the most common among different methods describing the aftershock behaviors.

The Gutenberg and Richter (1944) relation (G-R) describes the cumulative earthquake-size distribution in any region. The relationship between the frequency of occurrence and magnitude of aftershocks can be given by the following empirical equation:

$$\log_{10} N(M) = a - bM \tag{1}$$

where *N(M)* is the cumulative number of aftershocks with magnitudes equal/greater than *M*, *a* and *b*-values are positive constants. The *a*-value defines the earthquake activity level and shows significant changes from a region to another, because it depends on observation period and investigation area. The *b*-value describes the magnitude-frequency distribution of aftershocks, and tectonic structure of study region effects the spatial and temporal variations of *b*-value. The estimated *b*-value varies mostly from 0.6 to 1.4 (Wiemer and Katsumata 1999). Utsu (1971) also stated that *b*-values changes roughly between 0.3 to 2.0, depending on the study region. Frohlich and Davis (1993) suggested that the mean *b*-value in global scale can be given as equal to 1.0.

Aftershock occurrence rate as a function of time can be empirically described by the modified Omori law (MO). The number of aftershocks increases suddenly after a mainshock and then decreases with time after the mainshock according to the modified Omori law which can be formulated by a following empirical equation:

$$n(t) = \frac{K}{(t+c)^p} \tag{2}$$

where *n(t)* is the occurrence rate of aftershocks (number of aftershocks/day) per unit time, *t*-days after the mainshock. *K*, *p*, and *c* values are empirically derived positive constants which depend on the total number of events in the sequence and the activity rate in the earliest part of the sequence, respectively. *K*-value depends on the total number of aftershocks, *c*-value on the rate of activity in the earliest part of the sequences. The *c*-value varies between 0.02 and 0.5, and all the reported positive *c*-values result from incompleteness (Hirata 1969). Among these three parameters, *p*-value is the decay parameter and the most important. Utsu *et al*., (1995), Wiemer and Katsumata (1999) and Enescu and Ito (2002) said that *p*-value usually varies between 0.5 and 1.8 for different aftershock sequences.

Fracture systems are described by a power law, with a characteristic exponent called a fractal dimension, *Dc*-value, and this parameter has widely been used in seismology, especially to regional distribution of epicenters. Fractal dimension of the epicenter distribution of aftershocks can be modelled by using two-point correlation dimension, *Dc*, and correlation sum *C*(*r*) formulated by following equation (Grassberger and Procaccia 1983):

$$Dc = \lim_{r \to 0} [\log C(r) / \log r] \quad (3)$$

$$C(r) = 2N_{R<r} / N(N-1) \quad (4)$$

where $C(r)$ is the correlation function, r is the distance between two epicenters and N is the number of aftershocks pairs separated by a distance $R<r$. If the epicenter distribution has a fractal structure, following equation can be given:

$$C(r) \sim r^{Dc} \quad (5)$$

where Dc is the fractal dimension, more definitely, the correlation dimension. Fractal dimension varies from 0 to 2 related to the seismotectonically active regions. If Dc-value is close to 2, the earthquake epicenters are homogeneously distributed over a two-dimensional fault plane and the planar fractured surface are being filled-up. Fractal dimension might be estimated to avoid the possible unbroken fields, and these unbroken regions are suggested as potential seismic gaps to be broken in the future (Öncel *et al*., 1996).

Quantitatively, when the magnitude of aftershocks increases, their number declines exponentially. Expected number of aftershocks N (T_1, T_2) larger than M magnitude during the time from T_1 (starting time) to T_2 (ending time) is estimated by:

$$N(T_1, T_2) = \int_{T_1}^{T_2} \Lambda(M, s) ds = K \exp\{-b \ln 10 (M - M_{th})\} A(T_1, T_2) \quad (6)$$

where, K is a parameter from the MO law; b is a parameter of the G-R relationship and M_{th} is the magnitude not less than the magnitude of completeness (Ogata 1983). A (T_1, T_2) can be formulated as:

$$A(T_1, T_2) = \begin{cases} \dfrac{(T_2 + c)^{1-p} - (T_1 + c)^{1-p}}{1-p} & (p \neq 1) \\ \ln(T_2 + c) - \ln(T_1 + c) & (p = 1) \end{cases} \quad (7)$$

where c and p-values are constants from the MO formula. The probability Q of one or more aftershocks of M magnitude or larger occurring since the

mainshock, from the time T_1 to T_2 is found by Equations 8 and 9 (Reasenberg and Jones 1989):

$$Q = 1 - \exp\left\{ - \int_{T_1}^{T_2} \lambda(M, s) ds \right\} = 1 - \exp\{ - N(T_1, T_2) \} \tag{8}$$

$$Q = \begin{cases} 1 - \exp\left[\dfrac{-Ke^{-\beta(M - M_{th})}}{1-p} \left\{ \dfrac{1}{(T_2 + c)^{p-1}} - \dfrac{1}{(T_1 + c)^{p-1}} \right\} \right] & (p \neq 1) \\ 1 - \exp\left[-Ke^{-\beta(M - M_{th})} \{ \ln(T_2 + c) - \ln(T_1 + c) \} \right] & (p = 1) \end{cases} \tag{9}$$

In these formulations, *K*-value is approximately proportional to the total number of aftershocks; *p*-value represents the extent of time damping; *c*-value compensates for complex aspects immediately after the main shock, β represents the relationship of *b* and $\beta = b \ln 10$ =2.30*b*. The β is closely related to the number of small aftershocks/that of large aftershocks ratio and, its great value indicates relatively small number in large aftershocks. M_{th} is the magnitude of the smallest earthquake processed using the MO law or the G-R relation. It is premised that all aftershocks greater than M_{th} are observed without omissions. T_1 to T_2, which represent the starting and end of the time interval during the aftershock probability, is evaluated; both represent elapsed time following the mainshock. As a result, Equation 9 does not indicate an aftershock possibility that matches the conditions which occurs exactly once; it indicates the possibility of it which occurs more than one time.

4. Assessing the Aftershock Hazard Parameters and Discussions

A statistical evaluation of aftershock sequence of June 1, 2019 Korça earthquake was achieved by analyzing the space-time-magnitude distribution. Consequently, several seismotectonic parameters related to aftershock hazard evaluation were investigated. The use of complete data set for all magnitude sizes helps obtain reliable results, and especially estimate the *b*-value and *p*-value. As the first step, the minimum magnitude of completeness, *Mcomp*, based on the assumption of the G-R power law distribution of magnitudes can be estimated. *Mcomp* can be theoretically defined as the smallest magnitude that all the earthquakes are recorded. It can be defined as the minimum magnitude of complete reporting and means that *Mcomp* level contains 90% of the events (Wiemer and Wyss 2000). *Mcomp* changes systematically as a function of space and time, and particularly the time variations of *Mcomp* after the mainshock can produce erroneous *b* and *p*-value estimations. *Mcomp*

can be higher in the early part of the sequence since the small events fall within the coda of larger shocks. Thus, small events may not be located. The estimation of *Mcomp* is a quite significant step for all seismicity-based studies since the usage of the maximum number of aftershocks is necessary. The variations in *Mcomp* as a function of time for the aftershock sequence of June 1, 2019 Korça earthquake were plotted in Figure 3. We used a moving window technique and started from the origin time of the mainshock. *Mcomp* was estimated for samples of 10 events/window. Considering this number of aftershocks per window, an average magnitude was calculated for these selected events and this average value for each window was accepted as mean *Mcomp* for the time interval which covers that window. This process was repeated for each window until the end of catalog and each *Mcomp* value was attributed as the average value which covers the related time window. Thus, estimation of *Mcomp* value can be calculated as a function of time with an overlapping moving window approach by using maximum likelihood method. *Mcomp* changes between 3.0 and 4.0, relatively highest, at the beginning of the sequences (in the first ten hours), and then decreases to about between 1.5 and 2.5 in one hour after the mainshock. However, it decreases to about 2.0 within five days from the mainshock. We can easily see from Figure 3 that *Mcomp* changes from 1.0 to 2.0 after ten days from the mainshock. During the time interval of 110 days, 719 aftershocks were used for June 1, 2019 earthquake and, in order to understand how much the *Mcomp* changes hinge on the sample size, we tried the different sample sizes such as 25, 35, and 75 events/window and saw that the selection of the sample size does not affect the results. Consequently, the fluctuations in completeness plotted in the Figure 3 do not depend on the small sample size and *Mcomp* was selected as 1.8 in the estimation of *b*-value and *p*-value.

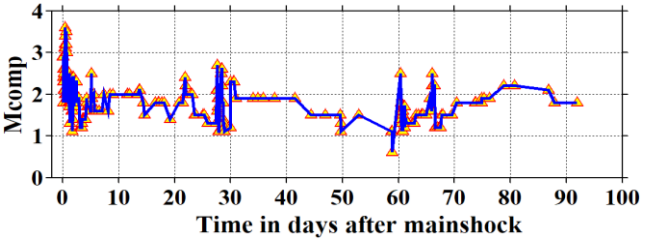

Fig. 3: Magnitude of completeness, *Mcomp*, as a function of time for the aftershock sequence of June 1, 2019 Korça earthquake. *Mcomp* was estimated for samples of 10 events/window with the moving window method.

The magnitude histogram of the aftershock sequence of the Figure 4 helps us see the changes in the number of aftershocks in different magnitude bands. Magnitudes of the aftershocks vary from 0.6 to 5.0 and show a decrease in

their numbers from the smaller to larger magnitudes. As seen in magnitude histogram, the size of the many aftershocks varies from 1.0 to 4.0 and a maximum was observed in M_L=1.8. There are 326 aftershocks with magnitude M_L<2.0, 196 aftershocks 2.0≤M_L<2.5, 104 aftershocks 2.5≤M_L<3.0, 83 aftershocks 3.0≤M_L<4.0, 10 aftershocks 4.0≤M_L and the aftershock with M_L=5.0 is the largest of all. Thus, the aftershock occurrences with magnitudes varying between 1.5 and 2.5 prevail in the aftershock region.

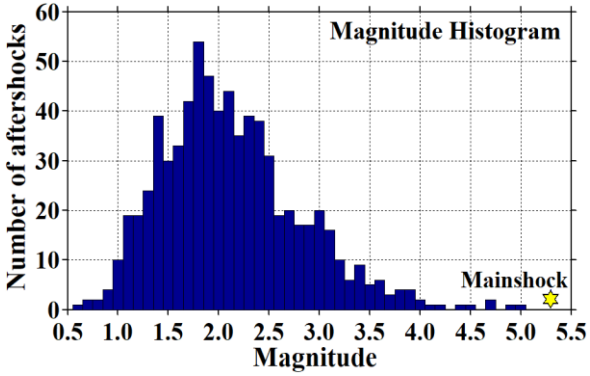

Fig. 4: Magnitude histogram of the aftershock sequence of June 1, 2019 Korça's earthquake.

The Figure 5 depicts the time histogram of the aftershock sequence for a better understanding of the changes in the number of aftershocks in different time intervals. There is a large aftershock activity in the first two days and the number of aftershocks in this time interval is about 280. There is also a decrease in the number of aftershocks after 10 days. Stableness can be clearly seen after the first month and, the average number of aftershocks after the first month is less than 10. However, there are some important increases in the number of aftershocks after 26 (92 events) and 59 (85 events) days. Thus, these types of evaluations can give preliminary results about the statistical properties of aftershock sequence which is associated with the aftershock probability evaluation and aftershock hazard in the Korça region.

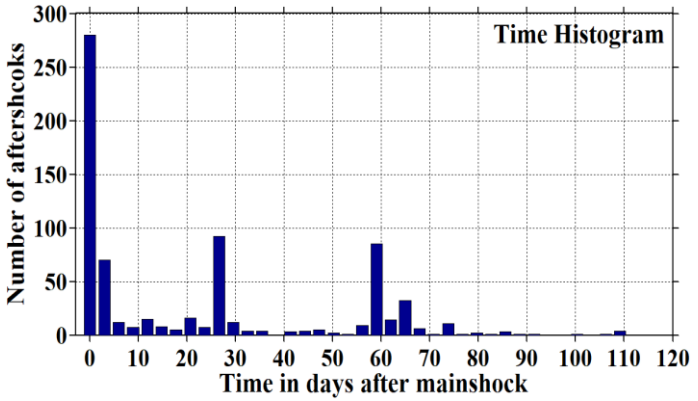

Fig. 5: Time histogram of the aftershock sequence of June 1, 2019 Korça's earthquake.

The principal application of aftershock probability evaluation techniques based on the statistical models clarifies the problem of determining whether it is or not possible to stably find the parameters (*K, c, p, b*) for aftershock activity immediately and correctly following a mainshock (Ogata 1983). If the average values of aftershock hazard parameters for the aftershock sequence are known, the existing values might be used correctly as preliminary data until the real data becomes available. Therefore, some scaling parameters obtained from the aftershock probability model combining the G-R and MO formulas were compared, and their application range was studied for the aftershock sequence of June 1, 2019 Korça's earthquake. We tested the confidence of the results for *b*-value and considered the effects of different *Mcomp* and upper limits of aftershock magnitudes. All results were given in the Table 2. Also, Figure 6 depicts the plot of frequency-magnitude distribution of the aftershocks for June 1, 2019 earthquake. *Mcomp* was taken as 1.8 considering the time variations in the Figure 3. The *b*-value, its standard deviation and *a*-value of G-R relation were estimated using this *Mcomp* with maximum likelihood method and *b*-value was calculated as 0.81±0.07. It is well known that estimation of *Mcomp* is a significant step for reliable results, and as the Table 2 reports, the *b*-value depends on *Mcomp* of the data. We made several tests employing different *Mcomp* (ranging from 1.8 to 2.5) and different upper limit of magnitudes (as stated in Bender 1983) to find the *b*-value. We saw that the *b*-value varies from 0.80 to 0.87 for different *Mcomp* values. In all the calculations, we computed *b*-value manually and we selected different *Mcomp* and upper limit of magnitudes. Since there are not large differences in *b*-values for different input parameters, we aimed to use the maximum number of aftershocks in the analyses. As shown in Table 2, *b*-value shows a characteristic in and around 0.8 and we

concluded that *b*=0.81±0.07 is more suitable for the Korça sequence. Frohlich and Davis (1993) stated that this *b*-value is smaller than the average value of *b*=1.0, and the smaller *b*-values may be related to the higher stress distribution, low heterogeneity degree of medium or high strain in this aftershock region of Albania in recent years.

Table 2. Some statistics for the estimation of *b*-value in G-R relation (in these calculations, mainshock was not included)

No	*Mcomp*	*Upper limit of magnitude*	Number of aftershocks used	*b*-value
1	1.8	5.0	494	0.81±0.07
2	2.0	5.0	393	0.82±0.05
3	2.5	5.0	197	0.84±0.04
4	1.8	4.3	488	0.80±0.05
5	2.0	4.3	387	0.82±0.04
6	2.5	4.3	191	0.87±0.03

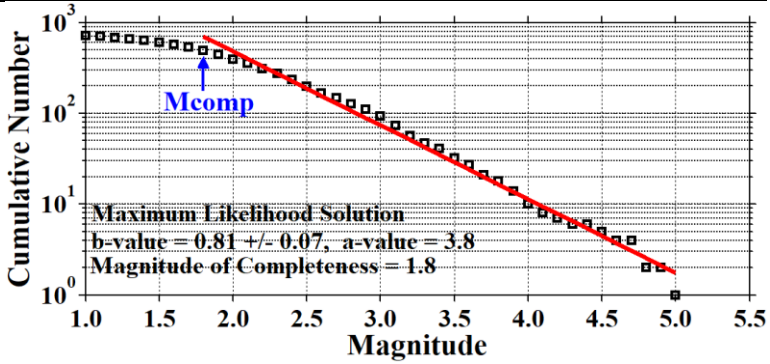

Fig. 6: Gutenberg-Richter relation of aftershock sequence of June 1, 2019 Korça's earthquake. *b*-value, its standard deviation, *Mcomp* as well as the *a*-value in the Gutenberg-Richter relation were given.

In order to estimate the decay parameters of aftershock occurrences, two significant threshold values must be adjusted to provide the completeness: (i) a minimum magnitude threshold *Mmin* and (ii) a minimum time threshold *Tstart* (T_1), i.e. excluding the first hours to days from the analysis. As a simple way, *Mmin* can be arranged for the shortest *Tstart*. However, this application uses the highest *Mcomp*, which is described for the earliest part of the aftershock occurrence (Wiemer and Katsumata 1999). For this reason, this selection decreases the available amount of data. For Korça aftershock sequence, *Mmin*=1.8 and *Tstart*=0.0014 were chosen to estimate the decay parameters of the modified Omori law. The *c*-value is measured in time units, days for example. After some earthquakes, there is some small delay in the

aftershock sequences. In some sequences, however, it can be observed a large incompleteness in the catalog at the very beginning of the aftershock sequence and therefore, an artificial large *c*-value may be estimated. These types of uncertainties on the calculations were tried to be removed by taking *Mmin*=1.8 and *Tstart*=0.0014. In this way, although the number of aftershocks was largely decreased, the earliest part of the sequence was included in the analyses and completeness was provided. In order to test the confidence of the results for *p* and *c*-values, we considered the effects of different *Mmin* and *Tstart*. All estimations are in Table 3 reported. Thus, for the estimation of decay parameters, 494 aftershocks with magnitude equal to and larger than 1.8 were used. Temporal decay rate of aftershock sequence was plotted in Figure 7. The *p*, *c* and *K*-values were estimated by using the maximum likelihood method for aftershocks with magnitude *Mcomp*≥*Mmin* and the occurrence rate was modeled by the MO formula. The *p*=0.96±0.04, relatively close to the global *p*-value 1.0, was calculated for aftershock sequence considering minimum magnitude *Mcomp*≥*Mmin*=1.8, T_1=0.0014 day. The *c*-value and *K*-value were calculated as 0.134±0.047 and 69.46±7.42, respectively. Since aftershock activity after the main shock shows a slow decay rate, relatively a small *p*-value was computed for the occurrence of aftershocks of June 1, 2019 Korça's earthquake. Utsu *et al*., (1995) pointed out that the *p*-value does not depend on *Mmin*, but the *c*-value depends heavily on the *Mmin* of the data. We made several tests to decay parameters for different *Mmin* (ranging from 1.8 to 3.0) and *Tstart* values (ranging from 0.0014 to 0.1). Results reported that the *p*-value varies from 0.94 to 1.23 for different *Mmin* and *Tstart*, and *c*-value between 0 and 0.155. Consequently, as shown in Table 3, *p*-value changes between 0.9 and 1.0 and, *c*-value is suggested to strongly relate to the *Mmin* in comparison with *p*-value.

The number of aftershocks may not be counted exactly at the beginning of a sequence when smaller aftershocks are often hidden by greater ones due to overlapping and therefore, too large *c*-value can be obtained. Utsu (1971) stated that *c*-value may be zero if all events can be counted. There are two ideas in relation to *c*-value: one is that *c*-value is actually 0 and all the reported positive *c*-values result from incompleteness in the early stage of an aftershock occurrence. The second idea is that positive *c*-value can be obtained (Enescu and Ito 2002). If *c*=0, *n* (*t*) in Equation (2) diverges at *t*=0. If the enlargement of the aftershock region occurs in an early stage, a relatively large *c*-value might be calculated (Utsu *et al*., 1995). Also, for the aftershock sequences following relatively small mainshocks, estimated *c*-values are generally small (*c*≤0.01 days). Hirata (1969) stated that *c*-value changes between 0.02 and 0.5 for the 1969 Shikotan-Oki earthquake (*M*6.9; from Utsu, 1969). Considering these detailed literature studies, we decided that the use of *Mmin*=1.8, *Tstart*=0.0014 for the estimation of decay parameters seems

better to fit the Korça aftershock sequence and, the results are in accordance with other studies.

A number of statistical models have been used to estimate the decay parameters of aftershocks and to describe the behavior of aftershock sequences since the first description by Omori (1894). Although alternative models such as Epidemic Type Aftershock Sequence (ETAS) model (Ogata, 1983), Marcellini (1997) approach, stretched exponential relaxation (Mignan, 2015), modified Omori law including a background rate term (Öztürk *et al*., 2008), etc., have been proposed to analyze the aftershock occurrences, different techniques have limited results relative to the MO law. Among different models, the MO law is one of the most effective approaches. Also, our results show that aftershock activity does not have a heterogeneous background seismicity pattern. Hence, and also considering the detailed statistics given in Table 3 (as seen in test 10), the simple modified Omori model appears suitable to describe the aftershock decay parameters of Korça earthquake sequence.

Table 3. Some statistics for the estimation of aftershock decay parameters

No	*Tstart* (T_1, day)	*Mmin*	Time interval (t, day)	Number of aftershocks used	*p*-value	*c*-value	*K*-value
1	0.05	1.8	0.050694≤t≤110.025	480	0.94±0.04	0.074±0.046	64.63±6.89
2	0.05	2.0	0.050694≤t≤110.025	380	0.95±0.04	0.054±0.042	50.98±5.75
3	0.05	2.5	0.054861≤t≤110.024	187	1.00±0.06	0.036±0.047	26.22±3.93
4	0.1	1.8	0.10208≤t≤110.025	460	0.94±0.04	0.078±0.068	64.97±7.97
5	0.1	2.0	0.10694≤t≤110.025	362	0.94±0.04	0.037±0.061	50.14±6.42
6	0.1	2.5	0.10694≤t≤110.024	179	0.99±0.06	0±0.058	25.52±4.13
7	0.01	1.8	0.011806≤t≤110.025	491	0.95±0.04	0.122±0.047	68.46±7.32
8	0.01	2.0	0.011806≤t≤110.025	390	0.97±0.04	0.102±0.044	54.31±6.14
9	0.01	2.5	0.011806≤t≤110.024	194	1.02±0.06	0.082±0.047	27.96±4.13
10	-	1.8	0.0013889≤t≤110.025	494	0.96±0.04	0.134±0.047	69.46±7.42
11	-	1.9	0.0013889≤t≤110.025	440	0.97±0.04	0.130±0.047	63.08±7.02
12	-	2.0	0.0013889≤t≤110.025	393	0.97±0.04	0.113±0.043	55.09±6.2
13	-	2.1	0.0013889≤t≤110.025	353	0.97±0.04	0.097±0.040	48.13±5.48
14	-	2.2	0.0013889≤t≤110.025	309	0.97±0.04	0.085±0.037	41.89±4.87
15	-	2.3	0.0013889≤t≤110.025	274	0.98±0.05	0.076±0.034	37.13±4.42
16	-	2.4	0.0013889≤t≤110.024	235	1.02±0.05	0.081±0.037	33.3±4.29
17	-	2.5	0.0013889≤t≤110.024	197	1.02±0.06	0.084±0.042	28.02±3.99
18	-	2.6	0.0013889≤t≤110.024	166	1.02±0.06	0.072±0.039	23.13±3.41
19	-	2.8	0.0013889≤t≤110.024	127	1.11±0.07	0.104±0.056	20.35±3.71
20	-	3.0	0.0013889≤t≤110.024	93	1.23±0.10	0.155±0.084	17.93±4.27

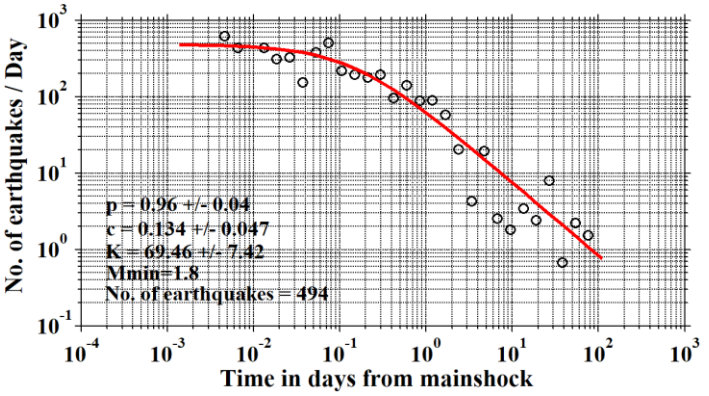

Fig. 7: Temporal decay rate of aftershocks per day for June 1, 2019 Korça's earthquake. *p*, *c* and *K*-values in the modified Omori formula, the minimum magnitude and the number of aftershocks used in the calculations are also given.

Fractal dimension of aftershock epicenter distributions is in Figure 8 plotted. *Dc*-value was estimated by fitting a straight line to the curve of mean correlation integral versus the event distance, *R* (km). *Dc*-value was computed as 1.89±0.07 for epicenter distribution of 719 aftershocks with 95% confidents interval by the least squares' regression. This log-log relation displays a clear linear range and scale invariance in the self-similarity statistics between 3.63 and 17.43 km. As stated above, fractal dimension may be used as a quantitative measure of heterogeneity degrees in fault geometry and stress. If there is an increasing complexity in the active fault system with higher *Dc*-value and smaller *b*-value, the stress release occurs on fault planes of smaller surface area (Öncel *et al*., 1996). Larger *Dc*-value is also sensitive to heterogeneity in magnitude distribution. *Dc*-value which was calculated as 1.89±0.07 in this work suggests that aftershocks are more clustered at larger scales or in smaller areas and, this large *Dc*-value may be a dominant structural feature for aftershock region. Since *Dc*-value is close to 2.0, we can imply that aftershocks of June 1, 2019 earthquake are homogeneously distributed. Thus, we can statistically describe and characterize the spatial distributions of aftershock epicenters and their fracture systems with fractal dimension.

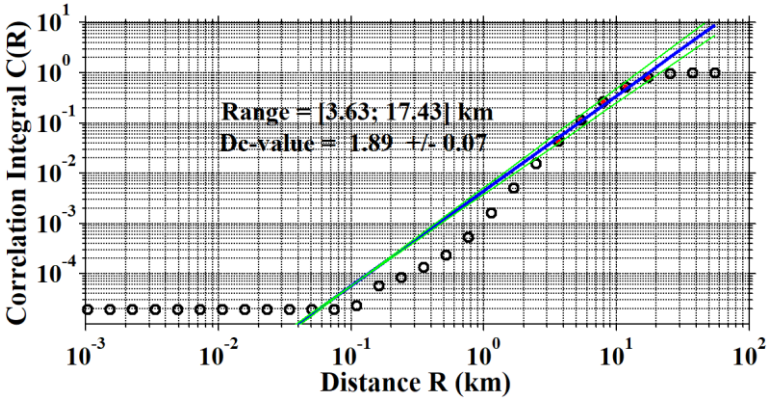

Fig. 8: Fractal dimension of aftershock epicenter distributions for June 1, 2019 Korça's earthquake. Scale invariance in the self-similarity statistics was indicated as "Range".

The *b*-value in G-R relationship was calculated by maximum likelihood estimation, because it yields a more robust estimate than least-square regression (Aki 1965). Parameters in the MO formula can be estimated accurately by the maximum likelihood solution, assuming that the seismicity follows a non-stationary Poisson process (Ogata 1983). The number of aftershocks (*N*), starting (T_1) and ending (T_2) times for the sequence, magnitude of completeness (*Mcomp*), *b*, *Dc*, *K*, *c*, and *p*-values for the aftershock sequence were given in Table 4.

The expected number of aftershocks and the occurrence probabilities of aftershocks for different magnitude levels are in Figure 9 and 10 shown, respectively. All the calculations were made considering the beginning and ending time intervals and the other hazard parameters of the aftershock sequence. The randomly chosen magnitude from aftershock sequence was considered as M_L=2.5 and estimated number of this magnitude size is in Figure 9 plotted. The maximum expected number of aftershocks for M_L=2.5 was computed as nearly 14. The occurrence probability of aftershock calculated for the largest aftershock M_L=5.0 and is in Figure 10 plotted. Probability of the largest aftershock was calculated as approximately 12 %. Thus, any other probabilities and expected numbers of a specific magnitude bands of aftershocks can be calculated from these analyses.

Table 4. Decay parameters and all statistics used in the aftershock probability evaluation

Earthquake	*N*	T_1 (day)	T_2 (day)	*Mcomp*	*b*-value	*Dc*-value	*K*-value	*c*-value	*p*-value
June 1, 2019	719	0.0014	110.025	1.8	0.81±0.07	1.89±0.07	69.46±7.42	0.134±0.047	0.96±0.04

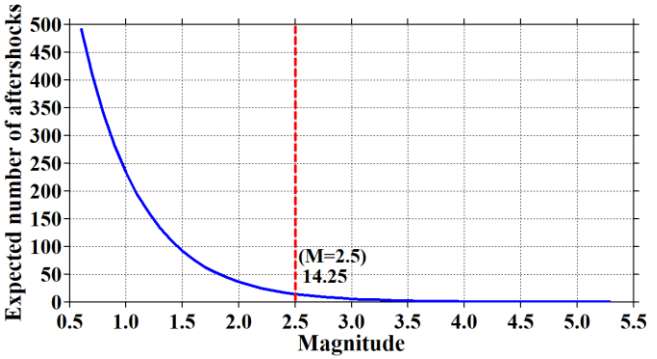

Fig. 9: Expected aftershock numbers for one or more shocks. Estimation was performed by using all aftershock hazard parameters as well as starting and ending times of the aftershock sequence.

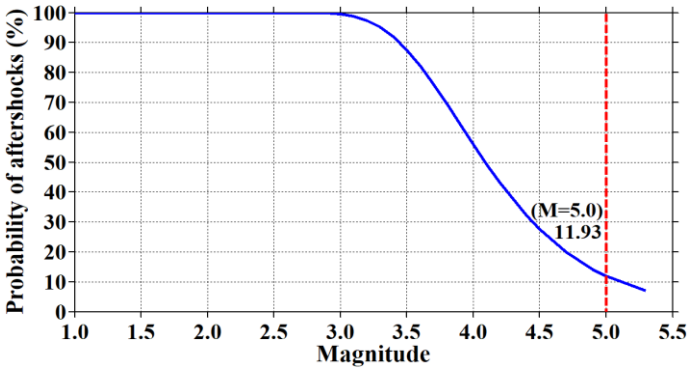

Fig. 10. Aftershock probabilities for one or more shocks. Estimation was performed by using all aftershock hazard parameters as well as the starting and ending times of the aftershock sequence.

5. CONCLUSIONS

First, the present paper aims to statistically evaluate the space-time-magnitude behaviors of June 1^{s}, 2019, M_L=5.3, Korça earthquake in details. Consequently, the *b*-value of the Gutenberg-Richter relation, *p*-value from the modified Omori law, *Dc*-value from fractal dimension were estimated along with the expected number of aftershocks and aftershock occurrence probability for different magnitude sizes. Aftershock catalog comprises 719 aftershocks. The *Mcomp* was estimated as 1.8 and the *b*-value was calculated as 0.81±0.07 with this *Mcomp*. This *b*-value smaller than 1.0 might be due to higher stress concentration, low heterogeneity degree of medium and high

strain in this aftershock area in recent years. Temporal decay parameters of aftershock sequence were calculated as p=0.96±0.04, c=0.134±0.047 and K=69.46±7.42 by fitting the data $Mcomp \geq Mmin$=1.8. This relatively small p-value refers that aftershock activity after the mainshock has a slow decay rate. From the estimated fractal dimension, Dc=1.89±0.07, it can be concluded that Korça aftershocks are heterogeneously distributed over a two-dimensional fault plane.

A magnitude level of M_L=2.5 was sampled for the estimation of expected number of aftershocks and the occurrence probability of the largest aftershock, M_L=5.0 was calculated during the aftershock period. Probability of the largest aftershock with M_L=5.0 was calculated as about 12 % and the expected numbers of aftershocks. The M_L=2.5 level was computed as nearly 14. As a remarkable fact, preliminary, reliable and correct space-time-magnitude evaluation and hazard assessments of the aftershock occurrences may be useful for the future studies on the implications on aftershock hazard and risk in any aftershock area. Also, these types of statistical results are a means to address disaster protection measurements and a perspective for the seismotectonic environment of the Korça aftershock region in Albania.

REFERENCES

Aki K. 1965. Maximum likelihood estimate of b in the formula $\log N = a - bM$ and its confidence limits. *Bulletin of Earthquake Research Institute of the University of Tokyo*. **43**: 237-239.

Aliaj Sh, Sulstarova E, Muço B, Koçiu S. 2000. Seismotectonic map of Albania at the scale 1:500.000. Instituti i Sizmologjisë Tiranë.

Aliaj Sh, Koçiu S, Muço B, Sulstarova E. 2010. Seismicity, seismotectonic and seismic hazard assessment in Albania. Published by Albanian Academy of Sciences.

Aliaj Sh, Meco S. 2018. Neotectonic map of Albania at the scale 1:200.000. Albanian Geological Survey, Tirana.

Ávila-Barrientos L, Zúñiga FR, Rodríguez-Perez Q, Guzmán-Speziale M. 2015. Variation of b and p values from aftershocks sequences along the Mexican subduction zone and their relation to plate characteristics. *Journal of South American Earth Sciences*. **63**: 162-171.

Bayrak Y, Öztürk S. 2004. Spatial and temporal variations of the aftershock sequences of the 1999 İzmit and Düzce earthquakes. *Earth Planets and Space*. **56** (**10**): 933-944.

Bender B. 1983. Maximum likelihood estimation of b values for magnitude grouped data. *Bulletin of the Seismological Society of America*. **73** (**3**): 831-851.

Chan CH, Wu YM. 2013. Maximum magnitudes in aftershock sequences in Taiwan. *Journal of Asian Earth Sciences*. **73**: 409-418.

Enescu B, Ito K. 2002. Spatial analysis of the frequency-magnitude distribution and decay rate of aftershock activity of the 2000 Western Tottori earthquake. *Earth Planets Space.* **54**: 847-859.

Frohlich C, Davis S. 1993. Teleseismic *b*-values: Or, much ado about 1.0. *Journal of Geophysical Research*. **98** (**B1**): 631-644.

Helmstetter A, Sornette D. 2003a. Diffusion of earthquake aftershock epicenters, Omori's law and generalized continuous-time random walk models. *Physical Review E,* **66** (**6**): 061104.

Helmstetter A, Sornette D. 2003b. Båth's law derived from the Gutenberg-Richter law and from aftershock properties. *Geophysical Research Letters*. **30** (**20**): 2069.

Hainzl S, Christophersen D, Rhoades D. Harte D. 2016. Statistical estimation of the duration of aftershock sequences. *Geophysical Journal International*. **205** (**2**): 1180-1189.

Felzer KR, Abercrombie R, Ekstrom G. 2003. Secondary aftershocks and their importance for aftershock forecasting. *Bulletin of the Seismological Society of America*. **93** (**4**): 1433-1448.

Grassberger P, Procaccia I. 1983. Measuring the strangeness of strange attractors. *Physics* **D9**: 189-208.

Gutenberg R, Richter CF. 1944. Frequency of earthquakes in California. *Bulletin of the Seismological Society of America*. **34**: 185-188.

Hamdache M, Peláez JA, Talbi A. 2013. Analysis of aftershock sequences in South and Southeastern Spain. *Physics and Chemistry of the Earth*. **63**: 55-76.

Hirata T. 1969. Aftershock sequence of the earthquake off Shikotan Island on January 29, 1968. *Geophysical bulletin of the Hokkaido University*. **21**; 33-43.

Koçiu S. 2005. Recent seismic activity in Albania and its features. Martinelli, G and Panahi, B. (eds.). Mud volcanoes, geodynamics and seismicity. NATO Science Series, series IV: Earth and Environmental Sciences. Springer, The Netherlands, 123-133.

Lay T, Wallace C. 1995. Modern global seismology. *International Geophysics*. Series 85.

Marcellini A. 1997. Physical model of aftershock temporal behavior. *Tectonophysics.* **277**: 137-146.

Nemati M. 2014. An appraisal of aftershocks behavior for large earthquakes in Persia. *Journal of Asian Earth Sciences*. **79**: 432-440.

Marsan D, Helmstetter A. 2017. How variable is the number of triggered aftershocks? *Journal of Geophysical Research: Solid Earth.* **122**: 5544-5560.

Mignan A. 2015. Modeling aftershocks as a stretched exponential relaxation. *Geophysical Research Letters.* **42**: 9726-9732,

Muço B. 1993. On the decay of aftershocks in Albania. The second Congress of Geophysics of Greece.

Narteau C, Shebalin P, Holschneider M. 2005. Onset of power law aftershock decay rates in southern California. *Geophysical Research Letters.* **32**: L22312.

Ogata Y. 1983. Estimation of the parameters in the modified Omori formula for aftershock frequencies by the maximum likelihood procedure. *Journal of Physics of Earth*. **31**: 115-124.

Ogata Y. 2001. Increased probability of large earthquakes near aftershock regions with relative quiescence. *Journal of Geophysical Research*. **106**; 8729-8744.

Ogata Y. 2010. Space-time heterogeneity in aftershock activity. *Geophysical Journal International*. **181**: 1575-1592.

Omori F. 1894. On after-shocks of earthquakes. *The Journal of the College of Science, Imperial University of Tokyo, Japan*. **7**: 111-200.

Ormeni Rr, Dushi E. 2009. Seismic characteristics of the Korca earthquake, August 28, 2008. *Journal Albanian Oil.*

Ormeni Rr, Öztürk S, Neritan Sh, Daja Sh. 2011. An application of the aftershock probability evaluation methods for recent Albania earthquakes based on Gutenberg-Richter and modified Omori models. International Balkans Conference on Challenges of Civil Engineering, BCCCE, 19-21 May 2011, EPOKA University, Tirana, Albania.

Ormeni Rr, Öztürk S. 2018. A statistical analysis on the aftershock sequence for July 3rd, 2017, border region of Macedonia-Albania (M_L=5.0) earthquake: Aftershock probability evaluation. *Journal of Natural and Technical Sciences*. **XXIII** (**47**): 95-110.

Ormeni Rr, Öztürk S. 2019. An appraisal on the aftershock characteristics of the July 4, 2018 earthquake, M_L=5.1, near Durrës, Albania. *Journal of Natural and Technical Sciences*, **XXIV** (**48**): 27-44.

Öncel AO, Main I, Alptekin A, Cowie P. 1996. Spatial variations of the fractal properties of seismicity in the Anatolian fault zones. *Tectonophysics***. 257**: 189-202.

Öztürk S, Çınar H, Bayrak Y, Karslı H, Daniel G. 2008. Properties of Aftershock Sequence of the 2003 Bingöl, M_D=6.4, (Turkey) Earthquake. *Pure and Applied Geophysics*. **165**(**2**): 349-371.

Öztürk S, Ormeni R. 2009. Aftershock probability assessment for the earthquake of September 6, 2009, Albania, based on the Gutenberg-Richter and modified Omori Formulae. *EMSC Newsletter*. **24**: 40-42 pp., France.

Öztürk S, Şahin Ş. 2019. A statistical space-time-magnitude analysis on the aftershocks' occurrence of the July 21th, 2017 M_W=6.5 Bodrum-Kos, Turkey, earthquake. *Journal of Asian Earth Sciences*. **172**; 443-457.

Reasenberg PA, Jones LM. 1989. Earthquake hazard after a mainshock in California. *Science*. **243**: 1173-1176.

Sulstarova E, Koçiaj S. 1975. The Albania Earthquake Catalog, Edition of Academy of Sciences of Albania.

Sulstarova E, Lubonja L. 1983. Karakteristikat e pasgoditjeve të tërmetit të 5 prillit 1979. Tërmeti i 15 prillit 1979. Shtëpia Botuese 8 Nëntori, 92-120.

Sulstarova E. 1985. Some aspects of Albania seismicity: VI Congress of the Carpatho-Balcan Geological Association, pp 135-140.

Shcherbakov R, Katsuichiro G, Armick I, Gail M. 2013. Aftershock statistics of major subduction earthquakes. *Bulletin of the Seismological Society of America*. **103** (**6**): 3222-3234.

Shebalin PN, Baranov SVJ. 2017. Rapid estimation of the hazard posed by strong aftershocks for Kamchatka and the Kuril Islands. *Journal of Volcanology and Seismology*. **11** (**4**): 295-304.

Utsu T. 1961. A Statistical study on the occurrence of aftershocks. *Geophysical Magazine*. **30**: 521-605, Tokyo, Japan.

Utsu T. 1971. Aftershock and earthquake statistic (III): Analyses of the distribution of earthquakes in magnitude, time and space with special consideration to clustering characteristics of earthquake occurrence (1). *Journal of the Faculty of Science, Hokkaido University*. Series VII (Geophysics), **3**: 379-441.

Utsu T, Ogata Y, Matsu'ura RS. 1995. The centenary of the Omori formula for decay law of aftershock activity. *Journal of the Physics of Earth*. **43**: 1-33.

Wei-Jin X, Jian W. 2017. Effect of temporal-spatial clustering of aftershocks on the analysis of probabilistic seismic hazard. *Chinese Journal of Geophysics*-Chinese Edition, **60** (**8**): 3110-3118.

Vere-Jones D. 1975. Stochastic models for earthquake sequences. Geophysical Journal International. **42** (**2**): 811-826.

Wiemer S, Katsumata K. 1999. Spatial variability of seismicity parameters in aftershock zones. *Journal of Geophysical Research*. **104** (**B6**); 13135-13151.

Wiemer S, Wyss M. 2000. Minimum magnitude of completeness in earthquake catalogs: Examples from Alaska, the Western United States, and Japan. *Bulletin of the Seismological Society of America*. **90** (**3**): 859-869.